Surface & Coatings Technology 347 (2018) 252–256

Contents lists available at ScienceDirect

Surface & Coatings Technology

journal homepage: www.elsevier.com/locate/surfcoat

Control and broadband monitoring of transparent multilayer thin films deposited by magnetron sputtering

A. Voronov[a], S.A. Atarah[b,*]

[a] Thin Film Centre, University of the West of Scotland, High Street, Paisley PA1 2BE, UK
[b] Department of Physics, University of Ghana, Legon, Ghana

ARTICLE INFO

Keywords:
Magnetron sputtering
Broadband monitoring
Thin transparent fil
Film deposition

ABSTRACT

A multilayer thin film deposition system has been developed that implements broadband process control and monitoring. Running on a simple algorithm, the system stringently controls the thickness of each of the multilayers thereby avoiding thickness error build up throughout the deposition process. The system which also has process monitoring capability can be implemented on any platform. Antireflection coatings deposited by the new system yielded spectral characteristics of commercial standards.

1. Introduction

Thin films have many and important applications. Their applications span across industry, health and research sectors. Materials coated with thin films or a cascade of thin films produce unique surface and optical properties not observable in conventional materials. Techniques for thin film coating include electron-beam evaporation with ion-beam assistance [1–3], ion beam sputtering [4,5] and reactive magnetron sputtering [6,7]. Magnetron sputtering is said to provide dense stable films and is the commonly preferred deposition method for the most demanding applications. It has been noted that without effective process control, magnetron sputtering processes can lead to poor run-to-run repeatability, poisoned target state [8], process drift and arcing [8–11]. The advent of nanoscience requiring applications in the nano-regime also places low tolerance limits on the precision for thin film coating. The above underpin the need for robust control and monitoring systems during magnetron sputtering.

Various systems exist for monitoring the thicknesses of thin films which include quartz crystal monitoring (quartz tooling), multi-wave ellipsometry and Real-time Spectroscopic Ellipsometry [12]. An extensively review by Kildemo et al. shows that besides their sensitivity to noise, most of these systems are unsuitable for multilayer films due to cumulative thickness errors [13].

A magnetron sputtering system with real time thickness control capability would be required in order to meet target optical characteristics of thin film deposited components.

In this paper, we demonstrate a broadband monitoring technique that has been integrated into a magnetron sputtering deposition system. The technique enables monitoring of layer thickness evolution by measuring the transmission spectrum of deposited thin films in situ. The transmission spectra of the evolving layers measured during deposition matched very well with the (calculated) theoretically expected characteristics at various stages of deposition. The system was used for depositing multilayer filters and anti-reflection coatings using Nb_2O_5 and SiO_2 and initial results have shown good matches with the targeted specifications. The spectral characteristics of filters deposited with same optical design specifications were reproducible and also showed no ageing effects. Simple modifications allowed the new monitor to be remotely controllable over a LAN network.

2. Experiment

2.1. Material and deposition set up

Anti-reflection (AR) coatings were deposited using Nb_2O_5 and SiO_2. Four layers were deposited (in alternation) on each side of BK7 glass substrate by microwave plasma-assisted pulsed-DC sputtering. Microwave power of 3 kW was applied and the frequency was 2.54 GHz. Fig. 1. is a schematic of the multilayer AR coating. The TFCalc software [14] was used to design the layering.

Details of the layers are given in Table 1.

The pulse D-C power and duty cycle of the system were preset at 5 kW and 70% respectively by the power supply unit. The deposition was done using a MicroDyn 40000 series magnetron sputtering system (DSI Inc.). Si and Niobium metal (Metal, Grey 99.98 wt% “SuperVac®” Evaporation grade as supplied by Testbourne LTD) were used as the target material whilst Ar and O_2 were used as sputtering and reactive gases respectively. Thus SiO_2 was the low (L) whilst Nb_2O_5 was the high

* Corresponding author.
E-mail addresses: a.voronov@uws.ac.uk (A. Voronov), saatarah@ug.edu.gh (S.A. Atarah).

https://doi.org/10.1016/j.surfcoat.2018.05.004
Received 25 October 2017; Received in revised form 4 April 2018; Accepted 3 May 2018
Available online 04 May 2018
0257-8972/ © 2018 Elsevier B.V. All rights reserved.

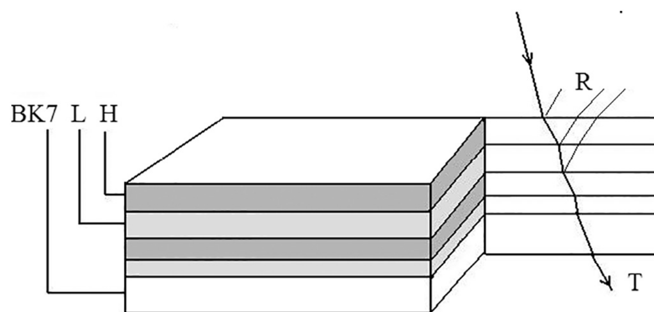

Fig. 1. Schematic of the anti-reflection coating. The schematic also suggests the transmittance (T) and suppressed reflectance (R) of a typical ray of light through the AR coating.

Table 1
Target details showing the thickness for each layer as obtained by the design software (TFCalc®).

Layer	Dielectric	Thickness (nm)	Layer	Dielectric	Thickness (nm)
Front side					
1	H	110.83	5	H	87.63
2	L	119.37	6	L	127.57
3	H	99.36	7	H	71.19
4	L	105.17	8	L	143.30
Back side					
1	H	100.20	5	H	79.14
2	L	115.44	6	L	145.01
3	H	92.71	7	H	183.51
4	L	103.85	8	L	78.60
Key	**H**	**Nb_2O_5**	**L**	**SiO_2**	

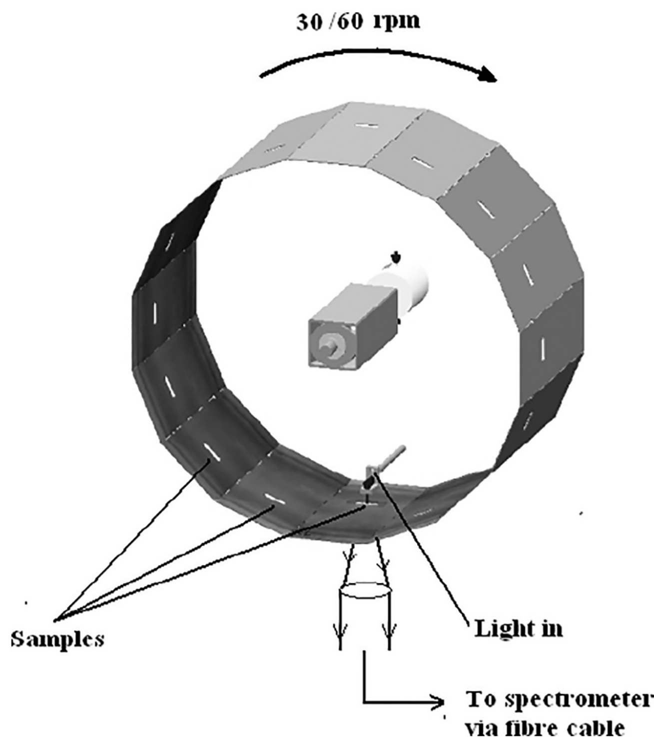

Fig. 2. Experimental setup for real time broadband monitoring and control of the thicknesses of samples on the revolving drum. Adapted with permission from earlier work [21].

(H) refractive index material. Both gases were fed in through a PC regulated mass flow controller by which the gas concentration was maintained. During deposition Ar: O_2 gas concentration ratio was typically maintained at 25 sccm: 14 sccm. This ratio is close to those recommended in a recent investigations on the effect of Ar/O_2 gas ratio on oxide multilayer film properties [15]. The total pressure in the chamber was about 5×10^{-3} Torr during deposition but deposition was not commenced till the chamber was pumped down to 5×10^{-6} Torr. In order to avoid out-gassing or spitting, a 10–15 min interval was allowed for pre-heating to slowly bring the target material up to deposition temperature. Twelve samples were deposited in one run and five runs were made from the same design with data collected on one representative sample during each run. For each process, the samples were arranged on a revolving drum in a chamber. Fig. 2 is a schematic of the system that was used. The drum was set to rotate at 60 rpm because at this speed deposited films showed more repeatable character over several runs compared to those deposited at the drum speed of 30 rpm. The layer deposition rate under these conditions was 2 Å/s.

Optical transmission spectra of deposited films were measured in the range 385–1100 nm using two systems: Peckin Elmer Lamda 19 and Scalar Technologies spectrometers. The latter spectrometer (Scalar) was used for the real time measurements whilst the former (Lamda 19) was used after deposition for the purpose of comparison. Both systems corroborated each other in the spectra obtained. The refractive index and absorption coefficients were obtained from the spectral data using the Cauchy method [16] which was integrated into the monitoring software. In order to verify repeatability of spectral characteristics of deposited films, the spectral data was periodically taken of random samples from different runs for comparison. Similar test measurements were also made after several weeks and the spectra compared with those of freshly deposited samples to check for any ageing effects.

2.2. Process monitoring and control

Glass substrates (of type BK7), on which films were deposited, were placed on holes on the rotating drum in the deposition chamber. A fibre optic cable, carrying white light, was introduced into the deposition chamber such that it run into the inner part of the drum directing the light to its outer part through the holes (on the drum). See Fig. 2. A geometrical optical system configured in the chamber just outside the drum collected the light from the fibre optic cable and relayed it to a diode array spectrometer (Scalar Technologies Ltd).

The geometrical optical arrangement was constructed in such a rigid way that any losses due to misalignment which have been reported [17] were minimized. By the arrangement, all samples (on the drum) cut the optical path normally in each revolution of the drum enabling the transmittance of the thin film samples to be measured during deposition. Both the spectrometer and the deposition system were connected to a PC. An in-house built software enabled concurrent process control and in situ measurement of film spectral data. During deposition the transmission spectrum of the sample and of the background reference were captured in each revolution of the drum. The background reference was essentially constant and so no stray reflections could affect the measured transmission spectrum. With systems that use rotation on same plane, a witness sample is needed.

The in-house developed software was the hub of the automation of the deposition system. In addition to implementing tight thickness requirements by the algorithm, the software also enabled remote control and monitoring over a LAN/Intranet connection. Details of the interrelations between the program modules and systems have been explained earlier [18].

3. Theory

3.1. Thickness monitoring

The point of focus of effort in this work was development of a system capable of repeatedly depositing stable layers of thin films with

minimum deviation from the required spectrum. In order to meet the target spectrum, layers must be deposited with minimal error in the thicknesses specified by the design software.

For thickness control the algorithm proposed by Wilbrandt et al. [19] was adopted. The algorithm follows the thickness, d^k, of the current layer being deposited with the object being to minimize as much as possible the difference, Δ, between the theoretically required thickness D^N and the actual deposited thickness d^N for the Nth layer. The layers are numbered 1, 2, 3…$k-1$, k, $k+1$, …, N.

Assume that $k-1$ layers were deposited within a window of j spectral points [$\lambda_1, \lambda_2, \lambda_3, \ldots \lambda_i, \ldots \lambda_j$]. Then the transmittance $T_M(\lambda_i)$ recorded at each spectral point λ_i is

$$T_M = T_M(\lambda_i), \quad i = 1, 2, 3, \quad ..j \tag{1}$$

The measured transmittance was then compared with the theoretically calculated transmittance. Computationally, the transmittance was obtained by considering the thickness d^k of the layer being deposited. Optical wave propagation in the medium can be described by a transfer matrix [20].

$$M_k = \begin{pmatrix} \cos(\varkappa d^k) & \frac{1}{\varkappa}\sin(\varkappa d^k) \\ -\varkappa\sin(\varkappa d^k) & \cos(\varkappa d^k) \end{pmatrix} \tag{2}$$

where k refers to the current layer and $\varkappa$ is the wave number. When transmission across a system of N stack of layers is considered, the system transfer matrix, M_s, becomes

$$M_s = M_N \cdot M_{N-1} \cdot M_{N-2} \cdots M_1. \tag{3}$$

The electric field transmitted across a layer can be expressed as

$$E(z) = tE_0 e^{i\varkappa_R z}. \tag{4}$$

where $E_0$is the amplitude of the wave at the boundary ($z = 0$)and the transmission amplitude t is given by (Born & Wolf [20])

$$t = 2i\varkappa_L e^{i\varkappa_L}\left[\frac{M_{11}M_{22} - M_{12}M_{21}}{-M_{12} + \varkappa_L\varkappa_R M_{12} + i(\varkappa_R M_{11} + \varkappa_L M_{22})}\right]. \tag{5}$$

In expression (5), M_{mn} refers to the components of the system transfer matrix whilst $\varkappa_R$ and $\varkappa_L$ are respectively the wave numbers in the medium to the right and left of the boundary. The transmittance was then obtained as $T_{cal} = |t|^2$.

The extent to which the measured transmittance agreed with T_{cal} was assessed at the current (kth) layer by use of a merit function, F, of the form.

$$F(d^k) = \sum_{i=0}^{j} [T_{cal}(d^k, \lambda_i) - T_M(\lambda_i)]^2; \quad 0 < d^k \approx D^k \tag{6}$$

Application of the merit function was facilitated by computing T_{cal}, at the same grid as the T_M. At each spectral point, the merit function depends only on the thickness of the current layer, d^k. Thus the function was vital in obtaining optimal thickness of the currently deposited layer. The minimum solution, d_{end}, of the merit function was used during deposition as the stopping criterion for the current layer:

$$d_{end}^k > D^k - \Delta \tag{7}$$

3.2. Algorithm implementation

The lab configuration for implementing the system was close to that described earlier [21]. Suppose a certain layer was being deposited. For any thickness, the transmittance was measured and compared with the calculated value so as to determine the thickness of the layer, d_{end}, for which merit function was acceptable (see Eq. (6)). Once the acceptable stopping criterion, d_{end}, was obtained, an interrupt signal was triggered which suspended the deposition system. At that instant the routine for the merit function was repeated several times to generate many values of the current layer thickness which was averaged to be the target thickness, d^k. Typically, for each layer, d^k was averaged from 15 generated values. The system was then returned from the suspended state after 30–45 s of delay and the monitoring advanced to the next layer for deposition, if the current layer was not the last one. As discussed below, for each layer in the design file, the program calculated and displayed the theoretical spectrum as a function of percentage completion for that layer. The current total thickness of the layer, where desired, was also used for calculating the spectrum. The software could be used to simulate the evolution of the film spectrum as well as closely follow the process development during deposition. The final spectrum of the last layer in the software repeatedly corresponded to the target spectrum as optically designed.

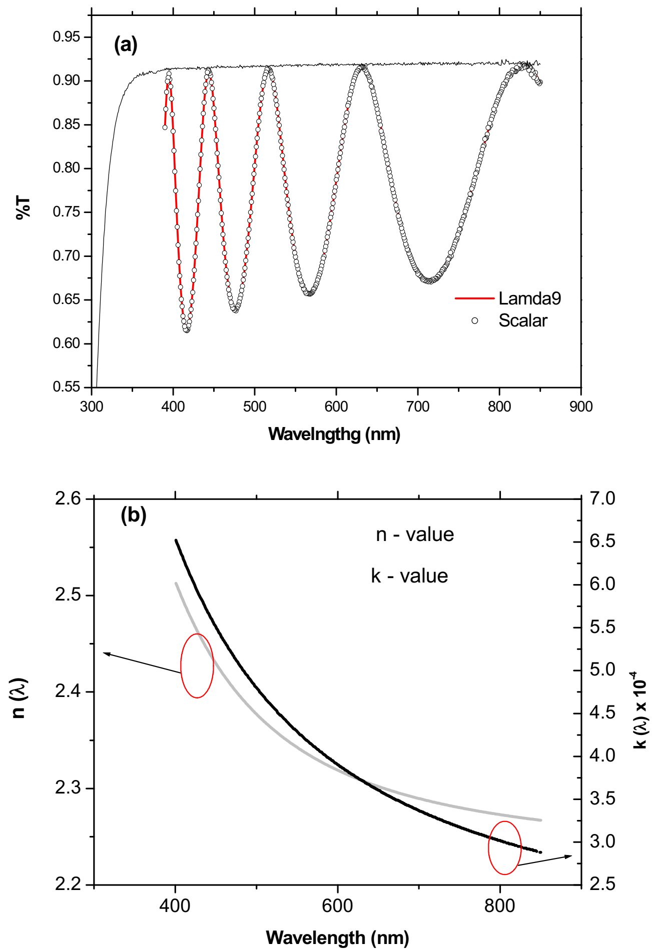

Fig. 3. (a) Transmission spectrum for a single layer of Nb_2O_5 as measured by two commercial spectrometers at room temperature.
(b) Refractive index and absorption coefficient variation with wavelength of Nb_2O_5.

4. Results

Fig. 3(a) shows the transmission spectrum of a single layer of Nb_2O_5 on BK7 glass substrate. Included in the figure for comparison is the transmission spectrum for the BK7 substrate only. Within the visible spectrum it can be seen that the maxima for the transmittance for Nb_2O_5 intersect that of the substrate indicating that deposition was homogeneous and nearly absorption free [22]. This was a pointer to the high quality of the target used for sputtering and is also an indication of optimal process conditions. Fig. 3(b) shows the dependence of the refractive index, $n(\lambda)$, and the absorption coefficient, $k(\lambda)$, on wavelength, i.e. $n-k$ characteristics. The $n-k$ data was extracted from the transmittance data by integrating the Cauchy method in the broadband

monitoring software. The $n - k$ values, as indicated by arrows in Fig. 3(b), were plotted for same wavelength. At 550 nm and 800 nm the refractive index values of 2.34 and 2.24 respectively match those obtained by other workers recently, [22,23].

It is well know that absorption within or below the order of 10^{-4} has a minor effect on transmittance. It can be observed from Fig. 3(b) that *k*-values were indeed of this order throughout the wavelength window of measurement. One can therefore say that with the process conditions fixed, absorption would have an insignificant effect on the results presented. The spectrum for the anti-reflection filter would thus be expected to be determined entirely by the precision with which the deposited film thicknesses conformed to the designed and also by the refractive index. Variation in the refractive index would affect transmittance and hence the thickness calculation. However, the refractive index would vary if there are changes in the composition of plasma (i.e. the ratio Nb_2O_5:SiO_2) [3] or in the deposition conditions. Under fixed process conditions therefore deposited components would have negligible errors in layer thicknesses and hence the repeatability of the spectra. In this work, the deposition pressure was fixed throughout the deposition process and the gas concentration was maintained by mass flow sensors controllers.

Fig. 4 shows the transmission spectrum as captured during the deposition of the first layer of the anti-reflection coating. Calculated spectra are shown for the layer as a function of completion stages at 20% intervals. For comparison with measured data, the spectra were also calculated for two values of layer thicknesses (91.30 nm and 118.71 nm) at which measurements were made during deposition. In Fig. 4, the measured spectral data are shown as symbols whilst lines represent calculated spectral data. It can be seen that there is an excellent agreement between the calculated and measured spectra. It suggests that the thicknesses deposited closely matched the values targeted. Similar spectra were observed for all layers throughout the process. It must be stated, though, that in few instances over coating and undercoating were observable but these often compensated each other. Infinitesimal deviations in the preceding layer thicknesses add up to later layer thicknesses. Thickness deviations can arise due to deposition history as follows. The merit function determines only the thickness of the current layer required to match the theoretical spectrum but the measured current spectrum is for the totality of layers already deposited. Thus, the function may under evaluate the current layer thickness if, due to positive residual errors, the measured thickness is more than the theoretical value. In such a case, a smaller value for the stopping criterion was obtainable resulting in under coating of the current layer. In a similar manner a layer may be over-coated.

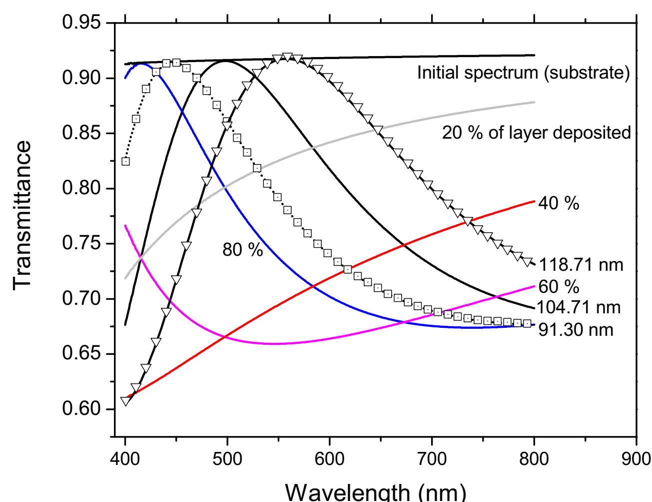

Fig. 4. Transmission spectrum as measured in situ and predicted by the algorithm.

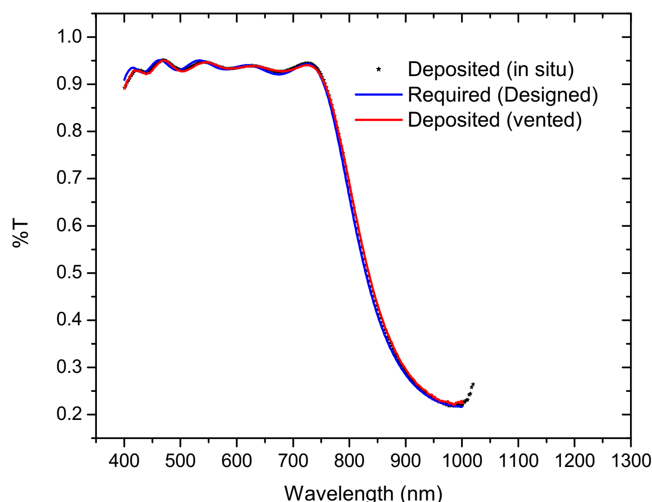

Fig. 5. The transmission spectrum of a deposited filter as measured in air (Vented) is compared with the spectral data for the theoretical design target (Design) and that taken in situ (Vacuum).

Under-coating and over-coating therefore compensate each other, minimizing over all thickness errors. Where over-coating or under-coating occurred, an error table indicating the deviation from the theoretical target layer thicknesses was kept. Five runs were made for the particular deposition presented and data on thickness error for each layer was recorded. Out of the total of 96 layers in one run, a mean value of 0.63 ± 0.21 nm was obtained for Δ. Thus on the average the thickness could be controlled to within 1 nm.

Fig. 5 is the spectrum of the anti-reflection coating taken after the final layer for one side was deposited but under process temperature and pressure. The theoretical target spectrum along with the spectrum of the same sample measured several weeks later is included in the figure for comparison. A good agreement with the target spectrum can be observed. It can be seen that age had shown little effect on the deposited filter. After backside coating the anti-reflection spectrum compared favourably with a commercial neutral density filter (part # NE201B, Thorlabs, Germany) for the visible regime.

5. Discussion

An important advancement realised by the new system is an enhanced process monitoring, i.e. real time availability of thickness and spectral information of deposited layers as well as strict thickness control leading to achievement of desired optical characteristics. A common problem in coating with multilayers of thin films is that errors in each of the layers add up towards the end, thereby making it hard to achieve the final target thickness and the desired spectral characteristics. The developed system though cannot be claimed to completely solve this problem but can minimize thickness errors to under 1 nm.

One more important advantage of the new deposition and monitoring over existing commercial systems is the response to (layer) process termination. Fig. 6 compares the spectra of two filters deposited from the same optical design but using the newly implemented monitoring system for one deposition (Fig. 6 (a)) and quartz monitoring for the other (Fig. 6 (b)). For clarity, data is shown from 650 nm for both cases. It can be seen that over all the spectra are more reproducible when monitored by the new system. With the quartz monitoring, the difficulty in reproducing the spectra especially at the edges is because of failure by quartz crystal monitor to consistently stop deposition at the defined layer thickness. Quartz tooling factor can vary [24]. Whilst the new broadband monitoring system uses the stopping criterion, d_{end}, to promptly interrupt the deposition process, quartz tooling factor changes with time. Other broadband monitoring systems control the layer

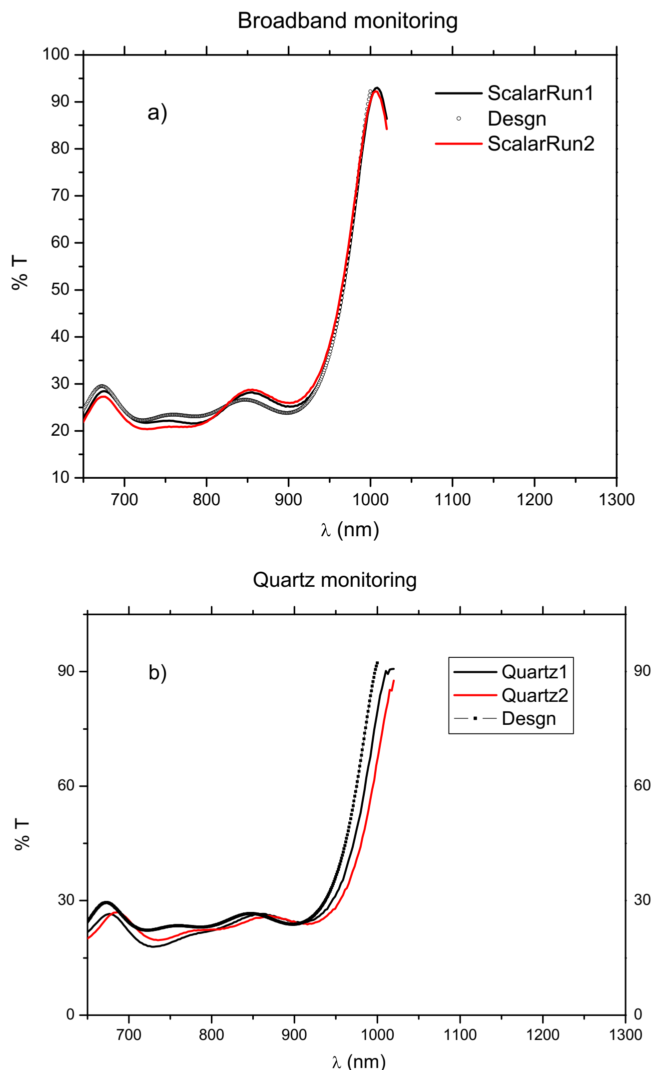

Fig. 6. The transmission spectrum of a gain flattening filter as deposited using (a) the new broadband monitor and (b) by quartz monitoring.

thickness by estimating the time required to deposit a certain layer from the deposition rate, the refractive index and the layer thickness [25]. In such systems the stopping criterion (time to deposit) depends on three factors each of which can cause an error in the thickness of the deposited layer. The deposition rate for our system at the set gas concentration was typical of those reported recently [22]. The system was tested for room temperature processing. The results are promising because low temperature depositions are known to be good for processing of low scattering loss optical coatings.

The broadband monitoring system has subsequently been applied to deposit output gain flattening filters, high reflection and antireflection components with repeatable characteristics.

The system in its current state is however limited to depositing only transparent thin films on transparent substrate as it relies on light transmitted through the layers for transmittance and thickness calculation. However, with a little modification, reflected light from samples can also be collected for process monitoring. Further works are underway to implement reflectance monitoring in the system and extend its applicability to non-transparent substrates.

6. Conclusions

A thin film coating instrument that embodies broadband process monitoring system has been developed. Using a compact algorithm, the transfer matrix method and basic computer connectivity, the system enables precise spectral measurements and real time determination of the thickness of a growing film. Implementation of the system was demonstrated by deposition of several anti-reflection coatings. Data collected from initial test runs using the new deposition and monitoring system shows that, on the average, the deviation from target layer thickness was controlled to 0.63 ± 0.21 nm. A comparison of transmission spectra of deposited filters as monitored by quartz and by the new broadband monitor shows how superior the latter system is in adhering to designed layer thicknesses during deposition. The monitoring was implemented across a LAN introducing flexibility to monitor the deposition system remotely.

Acknowledgement

The authors would like to acknowledge Dr. S. Song (University of the West of Scotland, UK) who was a research assistant at the Thin Film Centre at the time of the work for technical assistance.

References

[1] C. Xu, et al., Comparison of laser-induced damage in Ta_2O_5 and Nb_2O_5 single-layer films and high reflectors, Chin. Opt. Lett. 9 (2011) 013102.
[2] G. Abromavicius, et al., The microstructure and LIDT of Nb_2O_5 and Ta_2O_5 optical coatings, Proc. SPIE 6403 (2007) 640315.
[3] J. Sancho-Parramon, V. Janicki, H. Zorc, Compositional dependence of absorption coefficient and band-gap for Nb_2O_5–SiO_2 mixture thin films, Thin Solid Films 516 (2008) 5478.
[4] C.-C. Lee, J.C. Hsu, D.H. Wong, Low loss niobium oxides film deposited by ion beam sputter deposition, Opt. Quant. Electron. 32 (2000) 327.
[5] A. Melninkaitis, et al., Characterization of zirconia and niobia silica mixture coatings produced by ion-beam sputtering, Appl. Opt. 50 (2011) C188.
[6] S. Jakobs, et al., Characterization of metal-oxide thin films deposited by plasma-assisted reactive magnetron sputtering, Chin. Opt. Lett. 8 (2010) 73.
[7] F. Elsholz, et al., Roughness evolution in thin-film growth of SiO_2 and Nb_2O_5, J. Appl. Phys. 98 (2005) 103516.
[8] J. Musil, J. Vlcek, P. Baroch, Chapter 3 — magnetron discharges for thin films plasma processing A2, in: Y. Pauleau (Ed.), Materials Surface Processing by Directed Energy Techniques, Elsevier, Oxford, 2006, pp. 67–110.
[9] E. Hollands, D.S. Campbell, The mechanism of reactive sputtering, J. Mater. Sci. 3 (1968) 544.
[10] S. Venkataraj, O. Kappertz, M.W.R. Jayavel, Growth and characterization of zirconium oxynitride films prepared by reactive direct current magnetron sputtering, J. Appl. Phys. 92 (2002) 2461.
[11] M. Audronis, V. Bellido-Gonzalez, B. Daniel, Control of reactive high power impulse magnetron sputtering processes, Surf. Coat. Technol. 204 (2010) 2159.
[12] S. Marsillac, S.A. Little, R.W. Collins, A broadband analysis of the optical properties of silver nanoparticle films by in situ real time spectroscopic ellipsometry, Thin Solid Films 519 (2011) 2936–2940.
[13] M. Kildemo, B. Drivillon, Real-time control of the deposition of optical coatings by multiwavelength ellipsometry, Surf. Coat. Technol. 100-101 (1998) 480–485.
[14] M. Tilsch, et al., Design and Demonstration of a Thin-Film Based Gain Equalization Filter for C-Band, EDFAs NFOEC, 1999.
[15] X.F. Luo, Z.E. Ning, J.H. Wang, J.J. Yang, Y.J. Feng, J.L. Liao, Y.Y. Yang, K.M. Feng, N. Liu, M. Gong, Effects of Ar/O_2 ratio on preparation and properties of multilayer Cr_2O_3/α-Al_2O_3 tritium permeation barrier, Surf. Coat. Technol. 339 (2018) 132.
[16] R.S. Adve, T.K. Sarkar, Generation of accurate braodband information from narrowband data using the Cauchy method, Microwave Opt. Tecnhnol. Lett. 6 (10) (1993) 569–573.
[17] P.A.v. Nijnatten, Optical monitoring tools and strategies for controlling coating deposition in large area continuous coating processes, Thin Solid Films 502 (2006) 147–152.
[18] A. Voronov, F. Placido, I. Bain, In Situ Broadband Optical Monitoring and Characterization of Thin Films in 51st Annual Technical Conference Proceedings of the Society of Vacuum Coaters, (2008) (Chicago IL, USA).
[19] S. Wilbrandt, N. Kaiser, O. Stenzel, In-situ broadband monitoring of heterogeneous optical coatings, Thin Solid Films 502 (2006) 153–157.
[20] M. Born, E. Wolf, Principles of Optics: Electromagnetic Theory of Propagation, Interference and Diffraction of Light, Pergamon Press, Oxford, (1964).
[21] S. Atarah, et al., Integrated method for control and broadband monitoring of multilayer thin films, Optical Interf. Coating, Optical Society of America, Tucson, Arizona, USA, 2010.
[22] K. Juškevičius, et al., Fabrication of Nb_2O_5/SiO_2 mixed oxides by reactive magnetron co-sputtering, Thin Solid Films 589 (2015) 95–104.
[23] Ö.D. Coşkun, S. Demirel, The optical and structural properties of amorphous Nb_2O_5 thin films prepared by RF magnetron sputtering, Appl. Surf. Sci. 277 (2013) 35–39.
[24] H. Muramatsu, K. Maki, S. Tanabe, Basic characteristics of quartz crystal sensor with interdigitated electrodes, Anal. Chem. Res. 7 (2016) 23–30.
[25] L. Qipeng, M. Huang, S. Deng, G. Li, Fabrication of broadband antireflection coatings using wavelength-indirect broadband optical monitoring, Optik - International Journal for Light and Electron Optics 156 (2018) 325–332.